Research Article | Vol. 29, No. 8 / 12 April 2021 / Optics Express 11548
Optics EXPRESS

Transmitter and receiver impairment monitoring using adaptive multi-layer linear and widely linear filter coefficients controlled by stochastic gradient descent

MANABU ARIKAWA[1,2,*] AND KAZUNORI HAYASHI[2,3]

[1]System Platform Research Laboratories, NEC Corporation, 1753 Shimonumabe, Nakahara-ku, Kawasaki 211-8666, Japan
[2]Graduate School of Informatics, Kyoto University, Yoshida-honmachi, Sakyo-ku, Kyoto 606-8501, Japan
[3]RIKEN Center for Advanced Intelligence Project, 1-4-1 Nihonbashi, Chuo-ku, Tokyo 103-0027, Japan
[*]marikawa@nec.com

Abstract: We propose a monitoring method for individual impairments in a transmitter (Tx) and receiver (Rx) by using filter coefficients of multi-layer strictly linear (SL) and widely linear (WL) filters to compensate for relevant impairments where the filter coefficients are adaptively controlled by stochastic gradient descent with back propagation from the last layer outputs. Considering the order of impairments occurring in a Tx or Rx of coherent optical transmission systems and their non-commutativity, we derive a model relating in-phase (I) and quadrature (Q) skew, IQ gain imbalance, and IQ phase deviation in a Tx or Rx to the WL filter responses in our multi-layer filter architecture. We evaluated the proposed method through simulations using polarization-division multiplexed (PDM)-quadrature phase shift keying and a transmission experiment of 32-Gbaud PDM 64-quadrature amplitude modulation over a 100-km single-mode fiber span. The results indicate that both Tx and Rx impairments could be individually monitored by using the filter coefficients of adaptively controlled multi-layer SL and WL filters precisely and simultaneously, decoupled by chromatic dispersion and frequency offset, even when multiple impairments existed.

1. Introduction

Pursuing high spectral efficiency in optical fiber communication systems pushes adoption of advanced modulation formats such as higher-order quadrature amplitude modulation (QAM) [1–3]. Higher-order QAM is also used as a base format of probabilistic constellation shaping that enables flexible rate adaptation and high sensitivity approaching the Shannon limit [4–7]. High symbol rate has been tackled as well to increase the data rate per channel and reduce the number of components in entire wavelength-division multiplexed systems. Transmission experiments with a symbol rate beyond 100 Gbaud have recently been reported [8–10].

Signals with high spectral efficiency are generally susceptible to impairments. Since the emergence of digital coherent technology, distortion compensation can be flexibly implemented in digital signal processing (DSP), such as lumped chromatic dispersion (CD) compensation [11–13]. However, as the development of advanced modulation formats and high symbol rate progresses, impairments from imperfections in transmitter (Tx) and receiver (Rx) devices are becoming a limiting factor [3,6,7]. Therefore, compensation for and monitoring of Tx and Rx impairments are crucial for future high-speed optical fiber communication systems. Moreover, monitoring of individual impairments in Tx or Rx is required for diagnosing transmission systems.

In a Tx or Rx of optical fiber communication systems with coherent detection, timing skews between in-phase (I) and quadrature (Q) components, gain imbalance between IQ, and phase deviation of IQ from $\pi/2$ occur. Conventional DSP used in optical fiber communications

#416992 https://doi.org/10.1364/OE.416992
Journal © 2021 Received 8 Dec 2020; revised 1 Mar 2021; accepted 23 Mar 2021; published 30 Mar 2021

Optics EXPRESS

consists of filters with complex-valued coefficients and complex-valued signals as the phasor representation. Since these filters cannot treat IQ components independently, which is referred to as the strictly linear (SL) process in this context, they cannot compensate for IQ distortion under which I and Q components are differently distorted. To compensate for IQ distortion, multi-input multi-output (MIMO) filters with real-valued coefficients and real-valued signals of IQ components or equivalent complex-valued widely linear (WL) filters, in which complex-valued signals and their complex conjugates are inputs, are required [14]. Furthermore, several SL processes occurring through single-mode fiber (SMF) propagation, such as CD, polarization mode dispersion (PMD), and polarization rotation, cause mixing of IQ components; thus, this mixing should be addressed to compensate for IQ distortion occurring in a Tx or Rx [15].

To compensate for and monitor Tx and Rx impairments, various approaches have been proposed [14–20]. For Tx impairments, adaptive real-valued 2×2 MIMO filters with IQ components were applied after conventional CD compensation, polarization demultiplexing, and carrier recovery (CR) [16]. The amounts of Tx impairments, such as IQ skew, IQ imbalance, and IQ phase deviation, were estimated from the adaptive filter coefficients. For Rx impairments, an adaptive complex-valued 4×2 MIMO filter for compensating for both Rx impairments and polarization demultiplexing was used after independent CD compensation for IQ components to avoid IQ mixing, and Rx impairments were estimated from the filter coefficients [15]. These approaches focused on and treated blindly either Tx or Rx impairments. For both Tx and Rx impairments, ellipse correction was applied to compensate for and estimate Rx impairments, and k-means clustering based on blind phase search was applied for Tx impairments [17]. Adaptive filters have been used as well in compensating for Tx and Rx impairments. The Gram-Schmidt orthogonalization procedure (GSOP) [21] and an adaptive complex-valued 4×2 MIMO filter with independent CD compensation were used for Rx impairments, and cascaded adaptive real-valued 4×4 MIMO filters were used for Tx impairments [18,19]. An adaptive 4×2 MIMO filter with radius directed equalization and another adaptive 4×2 MIMO filter with decision-directed least mean square (LMS) after CR were applied for Rx or Tx impairments, respectively [20]. In these studies, Tx and Rx impairments were addressed individually.

The approach based on adaptive filters for Tx and Rx impairments is powerful in that it can compensate for and monitor IQ distortion including its frequency characteristics. However, adaptive filters for Tx and Rx impairment compensation in the previous studies were controlled locally by using their direct inputs and outputs. In this case, the first adaptive filter for Rx impairment compensation is imperfectly controlled under the condition where Tx impairments to be compensated for remain. This imperfect compensation affects the control of the following adaptive filter for Tx-impairment compensation as well.

To resolve the problem of this block-wise impairment compensation by using individual filters, we previously proposed a multi-layer SL&WL filter architecture where all the coefficients are adaptively controlled by stochastic gradient descent (SGD) with back propagation from the last outputs [22], similar to learning of multi-layer perceptrons in machine learning [23]. This multi-layer SL&WL filter architecture, while taking into account the order in which impairments occur, enables precise adaptive compensation for both Tx and Rx impairments under the accumulation of CD, polarization rotation, and frequency offset (FO) of a local oscillator (LO). In this multi-layer SL&WL filter architecture, the first and last WL filter layers serve as Rx and Tx impairment compensation. Although they are not controlled individually, the fact that both Tx and Rx impairments can be well compensated for in this architecture indicates that SL processes, such as CD and FO between Tx and Rx impairments, decouple them in terms of non-commutativity and that either is individually compensated for at the corresponding WL filter layer. In this study, we developed and evaluated a monitoring method for individual impairments in a Tx and Rx including IQ skew, IQ imbalance, and IQ phase deviation on the basis of filter coefficients of our adaptive multi-layer SL&WL filter architecture controlled by SGD with back propagation.

Optics EXPRESS

Considering the order in which IQ impairments occur in a Tx or Rx, we derive a model relating IQ skew, IQ imbalance, and IQ phase deviation to the corresponding WL filter responses in the multi-layer filter architecture in an organized manner. We evaluated the proposed method through simulations using 32-Gbaud PDM-quadrature phase shift keying (QPSK) and 100-km SMF transmission experiment of 32-Gbaud PDM-64QAM. The results indicate that both Tx and Rx impairments could be individually monitored using the WL filter coefficients precisely and simultaneously when multiple impairments existed.

2. Theory

We first review the models of Tx or Rx impairments including IQ skew, IQ imbalance, and IQ phase deviation by focusing on the order in which they occur in a Tx or Rx. We then derive the relations between IQ impairments and the WL filter responses that compensate for them. We consider the case with IQ modulation and coherent detection.

2.1. Models of Tx or Rx impairments

To consider the model of Tx or Rx impairments, it is beneficial to use the IQ component basis. The model for one polarization is enough for our purpose since two orthogonal polarizations are generally handled independently. Considering an input $x(t) = x_{\mathrm{I}}(t) + ix_{\mathrm{Q}}(t)$, where $x_{\mathrm{I}}(t)$ and $x_{\mathrm{Q}}(t)$ are the real-valued I and Q components, and an output $y(t) = y_{\mathrm{I}}(t) + iy_{\mathrm{Q}}(t)$, an arbitrary linear response is represented in the IQ component basis as

$$\begin{pmatrix} y_{\mathrm{I}}(t) \\ y_{\mathrm{Q}}(t) \end{pmatrix} = \int \begin{pmatrix} h_{\mathrm{II}}(\tau) & h_{\mathrm{IQ}}(\tau) \\ h_{\mathrm{QI}}(\tau) & h_{\mathrm{QQ}}(\tau) \end{pmatrix} \begin{pmatrix} x_{\mathrm{I}}(t-\tau) \\ x_{\mathrm{Q}}(t-\tau) \end{pmatrix} d\tau, \tag{1}$$

where h_{ij} $(i, j = \mathrm{I}, \mathrm{Q})$ are the real-valued linear response functions. The frequency domain representation of this equation is

$$\begin{pmatrix} Y_{\mathrm{I}}(\omega) \\ Y_{\mathrm{Q}}(\omega) \end{pmatrix} = \begin{pmatrix} H_{\mathrm{II}}(\omega) & H_{\mathrm{IQ}}(\omega) \\ H_{\mathrm{QI}}(\omega) & H_{\mathrm{QQ}}(\omega) \end{pmatrix} \begin{pmatrix} X_{\mathrm{I}}(\omega) \\ X_{\mathrm{Q}}(\omega) \end{pmatrix}. \tag{2}$$

We first consider the model of Tx impairments. Figure 1(a) shows the configuration of a conventional optical Tx with IQ modulation [24]. The outputs of a digital-to-analog converter (DAC) modulate a laser diode (LD) source. After mixing with $\pi/2$ phase shift of one side, they construct IQ components. In this configuration, IQ skew and IQ imbalance occur first, then IQ phase deviation occurs. Considering an arbitrary phase rotation of the generated optical signal, the frequency response of this model in the IQ component basis is described as

$$\begin{pmatrix} Y_{\mathrm{I}}(\omega) \\ Y_{\mathrm{Q}}(\omega) \end{pmatrix} = H_{\mathrm{Tx}} \begin{pmatrix} X_{\mathrm{I}}(\omega) \\ X_{\mathrm{Q}}(\omega) \end{pmatrix} = H_{\theta} H_{\mathrm{phase}} H_{\mathrm{imb}} H_{\mathrm{skew}} \begin{pmatrix} X_{\mathrm{I}}(\omega) \\ X_{\mathrm{Q}}(\omega) \end{pmatrix}, \tag{3}$$

where

$$H_{\mathrm{skew}} = \begin{pmatrix} \exp(i\omega\tau/2) & 0 \\ 0 & \exp(-i\omega\tau/2) \end{pmatrix}, \tag{4}$$

$$H_{\mathrm{imb}} = \begin{pmatrix} 1+a & 0 \\ 0 & 1-a \end{pmatrix}, \tag{5}$$

Optics EXPRESS

$$H_{\text{phase}} = \begin{pmatrix} 1 & \sin\varphi \\ 0 & \cos\varphi \end{pmatrix}, \tag{6}$$

and

$$H_{\theta} = \begin{pmatrix} \cos\theta & -\sin\theta \\ \sin\theta & \cos\theta \end{pmatrix}. \tag{7}$$

Here, τ, a, φ, and θ are the amounts of IQ skew, IQ imbalance, IQ phase deviation, and the global phase shift, respectively. They can be dependent on frequency, but we omit it for simplicity. H_{skew} and H_{imb} are mutually commutative but not commutative with H_{phase}. We can choose an arbitrary global phase shift as $\theta + \varphi/2$. Then, the frequency response of Tx impairments becomes

$$H_{\text{Tx}} = \begin{pmatrix} \cos(\varphi/2+\theta)(1+a)\exp(i\omega\tau/2) & \sin(\varphi/2-\theta)(1-a)\exp(-i\omega\tau/2) \\ \sin(\varphi/2+\theta)(1+a)\exp(i\omega\tau/2) & \cos(\varphi/2-\theta)(1-a)\exp(-i\omega\tau/2) \end{pmatrix}. \tag{8}$$

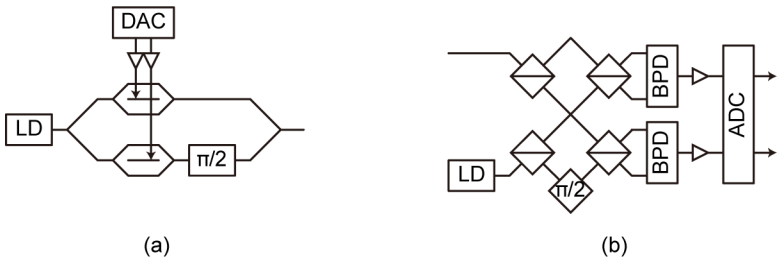

Fig. 1. Configurations of (a) optical Tx and (b) Rx with coherent detection. LD: laser diode, DAC: digital-to-analog converter, BPD: balanced photo-detectors, ADC: analog-to-digital converter.

Figure 1(b) shows the configuration of a conventional optical Rx with coherent detection [24]. The optical signal is mixed with an LO by a 90° optical hybrid, and IQ components are detected with balanced photo-detectors (BPDs). These signals are then converted into the digital domain by using an analog-digital converter (ADC) for demodulation DSP. In contrast to the Tx impairments shown in Fig. 1(a), IQ phase deviation comes first, then IQ skew and IQ imbalance occur in this Rx configuration. Based on the model of a 90° optical hybrid [25], IQ phase deviation affects IQ components as $H_{\text{phase}}^{\text{T}}$, where T is the transpose. Since an arbitrary phase shift to the optical signal is before IQ phase deviation, the frequency response of the Rx model in the IQ component basis is described as

$$\begin{pmatrix} Y_{\text{I}}(\omega) \\ Y_{\text{Q}}(\omega) \end{pmatrix} = H_{\text{Rx}} \begin{pmatrix} X_{\text{I}}(\omega) \\ X_{\text{Q}}(\omega) \end{pmatrix} = H_{\text{imb}} H_{\text{skew}} H_{\text{phase}}^{\text{T}} H_{\theta} \begin{pmatrix} X_{\text{I}}(\omega) \\ X_{\text{Q}}(\omega) \end{pmatrix}. \tag{9}$$

With an appropriate choice of an arbitrary phase shift, the frequency response of Rx impairments results in

$$H_{\text{Rx}} = \begin{pmatrix} \cos(\varphi/2-\theta)(1+a)\exp(i\omega\tau/2) & \sin(\varphi/2-\theta)(1+a)\exp(i\omega\tau/2) \\ \sin(\varphi/2+\theta)(1-a)\exp(-i\omega\tau/2) & \cos(\varphi/2+\theta)(1-a)\exp(-i\omega\tau/2) \end{pmatrix}, \tag{10}$$

which does not fall in the same response of Tx impairments, though they are similar, because of the order in which impairments occur.

Optics EXPRESS

2.2. Compensation for and monitoring of Tx/Rx impairments by using multi-layer SL&WL filters

In optical fiber communication systems, we should consider not only Tx and Rx impairments but other impairments such as CD, polarization rotation, and FO. Since Tx and Rx impairments are WL processes and are in general not commutative with these SL processes, the order in which to compensate for them should be considered.

Figure 2 shows the architecture of multi-layer SL&WL filters we have proposed to compensate for all the relevant linear impairments in optical fiber communications including Tx and Rx impairments [22]. The multi-layer filters are composed of five layers for Rx-impairment compensation, CD compensation, polarization demultiplexing, CR, and Tx-impairment compensation. All the filters are assumed finite impulse response filters with half-symbol spaced. Coefficients of all the filters can be controlled by SGD with back propagation on the basis of the loss function consisting of the last outputs since all the layers are differentiable in terms of their inputs and their filter coefficients, which is like the case with a parameterized unfolded function [26]. The first layer consists of two 2×1 WL filters for two polarizations to compensate for Rx impairments. The second layer consists of two 1×1 SL filters for CD compensation, the coefficients of which are treated as static. The third layer consists of a 2×2 SL MIMO filter for polarization demultiplexing and PMD compensation. The fourth layer consists of two 1×1 1-tap SL filters to compensate for the phase offset and FO. The fifth layer consists of two 2×1 WL filters to compensate for Tx impairments. The coefficients of the fourth layer are controlled by a decision-directed digital phase-locked loop using the last outputs. The coefficients of the first, third, and fifth layers are adaptively controlled by SGD with back propagation.

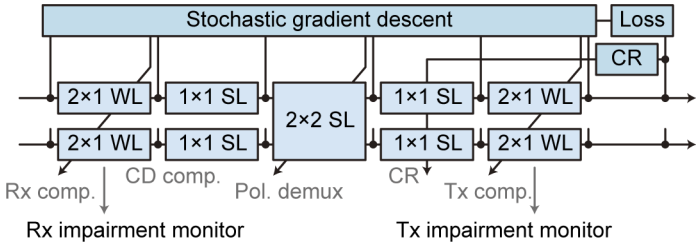

Fig. 2. Multi-layer SL&WL filters to compensate for all relevant linear impairments including Tx and Rx impairments where coefficients are adaptively controlled by stochastic gradient descent with back propagation from last outputs. WL: widely-linear, SL: strictly-linear, CR: carrier recovery.

The first and fifth WL filter layers are expected to serve as Rx- and Tx-impairment compensation in this multi-layer filters. Thus, their filter coefficients after adaptive control should contain information about Rx and Tx impairments if the adaptive filters work well. We now derive the relations between Tx and Rx impairments and the WL filter responses that compensate for them. For considering IQ impairments including IQ skew, IQ imbalance, and IQ phase deviation, using the IQ basis representation is advantageous. The complex-valued linear response functions of a 2×1 WL filter of h and h_*, with which the input-output relation is described as

$$y(t) = \int ((h(\tau))^* x(t-\tau) + (h_*(\tau))^* x^*(t-\tau)) d\tau, \tag{11}$$

are related to the 2×2 real-valued linear response functions of h_{ij} $(i,j = \mathrm{I}, \mathrm{Q})$ as [14]

$$\begin{pmatrix} h_{\mathrm{II}} & h_{\mathrm{IQ}} \\ h_{\mathrm{QI}} & h_{\mathrm{QQ}} \end{pmatrix} = \frac{1}{2} T^{\dagger} \begin{pmatrix} h^* & (h_*)^* \\ h_* & h \end{pmatrix} T, \tag{12}$$

Optics EXPRESS

where

$$T = \begin{pmatrix} 1 & i \\ 1 & -i \end{pmatrix}, \tag{13}$$

and $T^\dagger T = TT^\dagger = 2I$. The superscript $*$ is the complex conjugate, $\dagger$ is the Hermitian transpose, and I is the identity matrix. Using this relation, we can obtain the linear responses of a WL filter in the IQ basis representation and their corresponding frequency responses.

We represent the frequency responses of a 2×1 WL filter in the IQ basis representation as

$$W = \begin{pmatrix} W_{\mathrm{II}} & W_{\mathrm{IQ}} \\ W_{\mathrm{QI}} & W_{\mathrm{QQ}} \end{pmatrix}. \tag{14}$$

Ignoring noise contribution, the frequency responses of the first WL filter after the convergence of adaptive control in the IQ basis representation $W^{[1]}$ are expected to satisfy $W^{[1]} = gH_{\mathrm{Rx}}^{-1}$ with a certain complex-valued gain g. Assuming this relation, extracting IQ skew τ, IQ imbalance a, and IQ phase deviation φ occurring in an Rx from the coefficients of the first WL filter comes down to nonlinear simultaneous equations. The solutions are provided in a heuristic manner as follows. We consider these four values, which are independent on the global phase shift of θ, as

$$A^{[1]} = W_{\mathrm{II}}^{[1]} W_{\mathrm{QQ}}^{[1]} - W_{\mathrm{QI}}^{[1]} W_{\mathrm{IQ}}^{[1]}, \tag{15}$$

$$B^{[1]} = W_{\mathrm{II}}^{[1]} W_{\mathrm{QQ}}^{[1]*} - W_{\mathrm{QI}}^{[1]} W_{\mathrm{IQ}}^{[1]*}, \tag{16}$$

$$C^{[1]} = W_{\mathrm{QI}}^{[1]} W_{\mathrm{QQ}}^{[1]} + W_{\mathrm{II}}^{[1]} W_{\mathrm{IQ}}^{[1]}, \tag{17}$$

$$D^{[1]} = \sqrt{\frac{|W_{\mathrm{II}}^{[1]}|^2 + |W_{\mathrm{QI}}^{[1]}|^2}{|W_{\mathrm{IQ}}^{[1]}|^2 + |W_{\mathrm{QQ}}^{[1]}|^2}}. \tag{18}$$

By using these values, we can obtain

$$a_{\mathrm{Rx}} = \frac{1 - D^{[1]}}{1 + D^{[1]}}, \tag{19}$$

and

$$\varphi_{\mathrm{Rx}} = \tan^{-1}\left(-\frac{C^{[1]}}{A^{[1]}}\right). \tag{20}$$

If IQ phase deviation φ is small and the variation of IQ skew τ over frequency is slow,

$$\tau_{\mathrm{Rx}} = -\frac{d}{d\omega} \arg(B^{[1]}). \tag{21}$$

Similarly, assuming $W^{[5]} = gH_{\mathrm{Tx}}^{-1}$ for Tx impairments, we obtain

$$A^{[5]} = W_{\mathrm{II}}^{[5]} W_{\mathrm{QQ}}^{[5]} - W_{\mathrm{IQ}}^{[5]} W_{\mathrm{QI}}^{[5]}, \tag{22}$$

$$B^{[5]} = W_{\mathrm{II}}^{[5]} W_{\mathrm{QQ}}^{[5]*} - W_{\mathrm{IQ}}^{[5]} W_{\mathrm{QI}}^{[5]*}, \tag{23}$$

$$C^{[5]} = W_{\mathrm{IQ}}^{[5]} W_{\mathrm{QQ}}^{[5]} + W_{\mathrm{II}}^{[5]} W_{\mathrm{QI}}^{[5]}, \tag{24}$$

$$D^{[5]} = \sqrt{\frac{|W_{\mathrm{II}}^{[5]}|^2 + |W_{\mathrm{IQ}}^{[5]}|^2}{|W_{\mathrm{QI}}^{[5]}|^2 + |W_{\mathrm{QQ}}^{[5]}|^2}}, \tag{25}$$

Optics EXPRESS

and

$$a_{\mathrm{Tx}} = \frac{1 - D^{[5]}}{1 + D^{[5]}}, \tag{26}$$

$$\varphi_{\mathrm{Tx}} = \tan^{-1}\left(-\frac{C^{[5]}}{A^{[5]}}\right), \tag{27}$$

$$\tau_{\mathrm{Tx}} = -\frac{d}{d\omega}\arg(B^{[5]}). \tag{28}$$

Using their relations, we can monitor each of Tx and Rx impairments individually from the coefficients of the WL filters in the multi-layer SL&WL filters if the adaptive control by SGD with back propagation goes well.

3. Simulation results

We first evaluated the proposed monitoring method for individual Tx and Rx impairments from the coefficients of the multi-layer SL&WL filters through numerical simulations. We used a 32-Gbaud PDM-QPSK signal with a root raised cosine filter, where a roll off factor of 0.1, was transmitted over a 100-km SMF and received with coherent detection. On the basis of the above impairment model described in Section 2.1, IQ skew, IQ imbalance, and IQ phase deviation were imposed in the Tx and/or Rx. Only CD was given in SMF transmission. We assumed no laser phase noise and FO at first. The received optical signal-to-noise ratio (OSNR) was set to 30 dB/0.1 nm by adding white Gaussian noise. DSP was applied to the received signals sampled by two-fold oversampling after coherent detection.

In DSP, the received signals were first normalized as complex-valued signals for two orthogonal polarizations then resampled to two-fold oversampling based of the timing error [27]. After matched filtering, the above-mentioned five-layer adaptive multi-layer SL&WL filters were applied. The tap lengths of the filters were 61 taps for CD compensation (the second layer), 21 taps for polarization demultiplexing (the third layer), and five taps to compensate for Tx/Rx impairments (the first and fifth layers). The filter coefficients of the second layer were set to compensate for CD and did not updated. The filter coefficients at the center tap of the main diagonal position in the first, third, and fifth layers were initialized as one and the rest were set to zero. To monitor IQ impairments in a Tx and Rx, the transmitted IQ components should be identified. Therefore, the constant modulus algorithm (CMA) and decision directed LMS are not suitable since they include a certain phase ambiguity that results in the exchange of IQ components. The loss function based on data-aided LMS was thus used for adaptive control with SGD to avoid the uncertainty of the IQ components. In this simulation, the transmitted pattern was regarded as a training sequence for simplicity. The step sizes of the update were 10^{-4} for the first and fifth layers and 10^{-3} for the third layer.

After convergence of the adaptive filter control, the WL filter coefficients of the first layer were converted to the IQ basis representation then converted in the frequency domain by the fast Fourier transform. The amounts of IQ skew, IQ imbalance, and IQ phase deviation in the Rx were estimated using the previous equations described in Section 2.2. The values of the frequency components of 0 Hz were evaluated. Derivative was replaced with the finite difference between the components of 0 Hz and $\Delta\omega/(2\pi) = 12.8$ GHz. IQ skew, IQ imbalance, and IQ phase deviation in the Tx were estimated in a similar manner with the WL filter coefficients of the fifth layer.

We first evaluated the performance of compensation and impairment monitoring under the condition where only one of the impairments in the Tx and Rx was imposed. IQ skew, IQ imbalance, and IQ phase deviation of X polarization in the Tx or Rx were swept from −5 to +5 ps, −0.5 to 0.5, −10° to +10°, respectively. Figure 3 shows the results of the averaged error vector magnitude (EVM) over two polarizations after the multi-layer SL&WL filters. As a reference,

Optics EXPRESS

the results where only CD compensation, polarization demultiplexing by a 2×2 MIMO filter, and CR were carried out are shown in this figure (referred to as 2×2 SL). In addition, the results where a 4×2 WL MIMO filter was used instead of a 2×2 MIMO filter of 2×2 SL are shown for comparison (referred to as 4×2 WL). Regarding IQ skew and IQ phase deviation in the Tx or Rx, an almost constant EVM was obtained after using the multi-layer SL&WL filters while EVM degraded in the case of 2×2 SL as the impairment increased. EVM after the multi-layer SL&WL filters became worse with IQ imbalance in the Tx since it distorted added Gaussian noise, though compensation still worked. These results indicate that the multi-layer SL&WL filters could compensate for each of Tx and Rx impairments. In the case of 4×2 WL, only Tx impairments could be compensated since CD was included and FO and phase noise were not included.

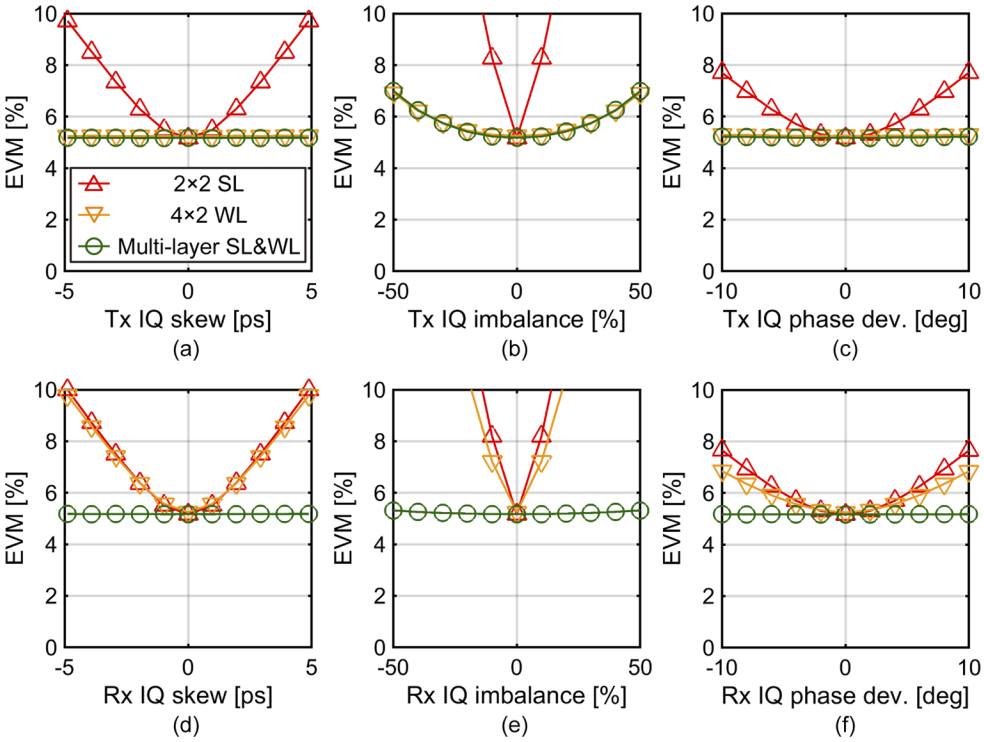

Fig. 3. Simulation results of EVM with (a) Tx IQ skew, (b) Tx IQ imbalance, (c) Tx IQ phase deviation, (d) Rx IQ skew, (e) Rx IQ imbalance, and (f) Rx IQ phase deviation.

The results of the impairment estimation for IQ skew, IQ imbalance, and IQ phase deviation in the Tx and Rx by using the converged WL filter coefficients of the multi-layer SL&WL filters are shown in Fig. 4. We can confirm that the imposed impairments and estimated ones agreed well.

We then evaluated the impairment monitoring with our method under the condition where multiple impairments were imposed simultaneously. IQ skew, IQ imbalance, and IQ phase deviation of X and Y polarization in the Tx and Rx were random values of a zero-mean Gaussian distribution with a standard deviation of 3 ps (10% of the symbol duration), 0.1, and 5°, respectively. Random rotation of the polarization state was also added in SMF transmission in addition to CD. The LO phase noise of the linewidth of 100 kHz was included. Figure 5 shows the results for monitoring the impairments of X polarization with 1000 random realizations of multiple impairments. The monitored values are plotted on the left axis, and the monitored errors from the imposed amounts are plotted on the right axis. Similar results were obtained for Y polarization, though they are not shown here. Similar to the results where only one of the

Optics EXPRESS

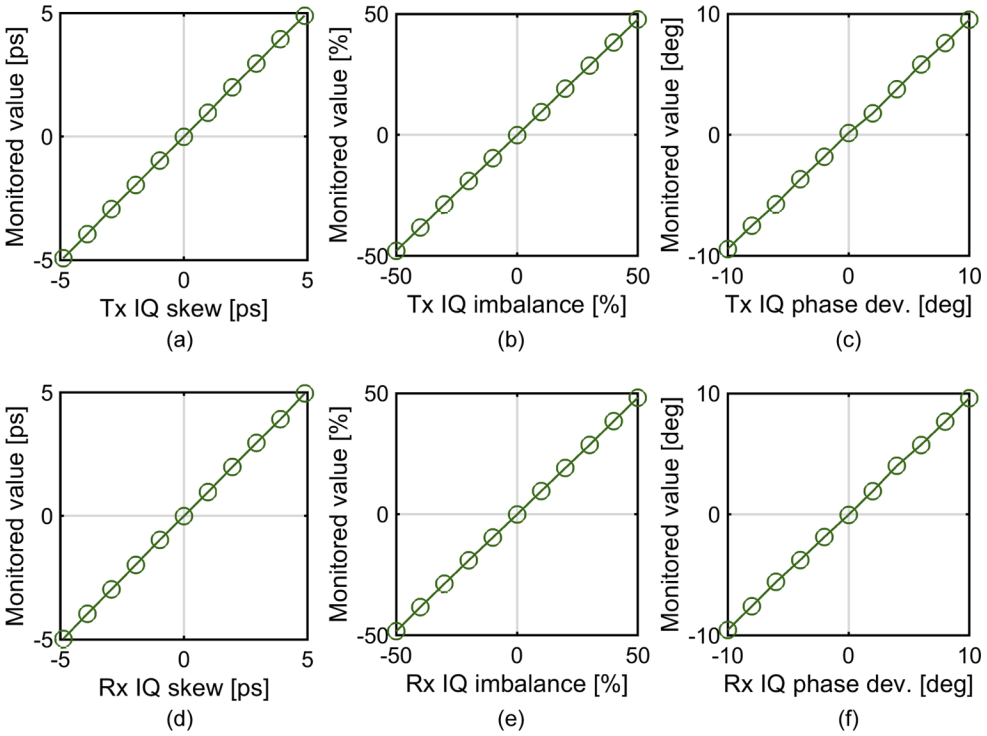

Fig. 4. Simulation results of impairment monitoring for (a) Tx IQ skew, (b) Tx IQ imbalance, (c) Tx IQ phase deviation, (d) Rx IQ skew, (e) Rx IQ imbalance, and (f) Rx IQ phase deviation.

impairments was imposed, as shown in Fig. 4, the imposed impairments and estimated values agreed well in this case where multiple impairments were imposed simultaneously. In accordance with the monitored error, the monitored values were biased due to the nonlinear relations to the WL filter coefficients, while they were small within about ±0.2 ps, ±0.02, and ±1° for IQ skew, IQ imbalance, and IQ phase deviation, respectively. The results indicate that the impairments in both Tx and Rx could be individually monitored from the WL filter coefficients precisely and simultaneously when multiple impairments existed.

Optics EXPRESS

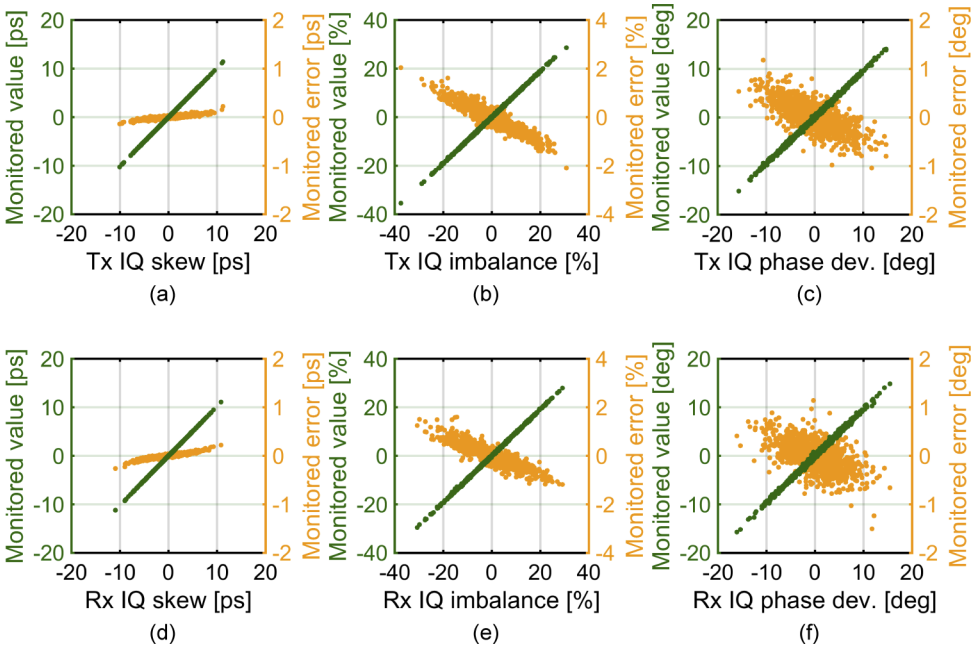

Fig. 5. Simulation results of impairment monitoring under random multiple impairment conditions for (a) Tx IQ skew, (b) Tx IQ imbalance, (c) Tx IQ phase deviation, (d) Rx IQ skew, (e) Rx IQ imbalance, and (f) Rx IQ phase deviation. Results for 1000 random realizations of multiple impairments are plotted in each figure.

4. Experimental results

Finally, we evaluated the proposed monitoring method for individual impairments in a Tx and Rx from the coefficients of the multi-layer SL&WL filters in a transmission experiment of 32-Gbaud PDM-64QAM over a 100-km SMF span. A schematic diagram of the experimental setup is shown in Fig. 6, which is a similar configuration to that in our previous study [22]. The 32-Gbaud PDM-64QAM was generated by modulating a laser source at the frequency of 193.3 THz having a linewidth of about 100 kHz with waveforms from a four-channel DAC at the sampling rate of 92 GS/s with a vertical resolution of eight bits. Transmitted data were 16 frames of low-density parity-check code for DVB-S2 with a frame length of 64,800 and code rate of 4/5 while random bits were loaded to their payload. These data were mapped to PDM-64QAM with Gray mapping. Pilot symbols of QPSK were inserted every 15 symbols to execute a pilot-based data-aided LMS. Due to the restriction of the data length that can be handled with the DAC used in the experiment, an overhead of QPSK symbols was inserted, which resulted in about 8% overhead in total with the pilot. The inserted QPSK symbols were set to any of the outer symbol points of 64QAM. The data were upsampled to two-fold oversampling, and a root-raised cosine filter with a roll-off factor of 0.1 was used. After using a pre-compensation filter to calibrate the frequency characteristic in Tx devices, the data for the IQ of each polarization were resampled to 92 GS/s to be generated with the DAC.

A 32-Gbaud PDM-64QAM signal was transmitted to a 100-km SMF after low-speed polarization scrambling with a speed of 10 $\times 2\pi$ rad/s. The span input optical power was set to 0 dBm. After 100-km SMF transmission, amplified spontaneous emission was added to set the OSNR to 30 dB/0.1 nm. The received optical signal was amplified using an erbium-doped fiber amplifier and filtered using an optical bandpass filter having a 3-dB bandwidth of 50 GHz. The optical signal was received using a polarization-diversity coherent receiver with a LO source having a

Optics EXPRESS

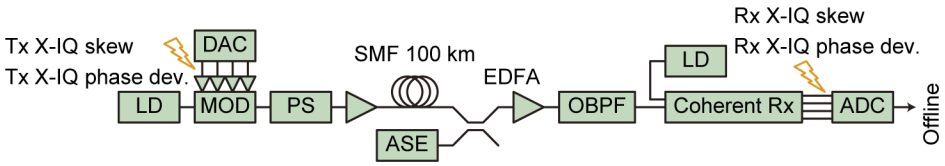

Fig. 6. Experimental setup of 32-Gbaud PDM-64QAM transmission over 100-km SMF span. LD: laser diode, DAC: digital-to-analog converter, MOD: modulator, PS: polarization scrambler, SMF: single-mode fiber, ASE: amplified spontaneous emission, EDFA: erbium-doped fiber amplifier, OBPF: optical bandpass filter, ADC: analog-to-digital converter.

linewidth of about 100 kHz. The laser sources for the signal and LO were free running. The FO was about 60 MHz on average, and its standard deviation was about 90 MHz. The four outputs of the coherent receiver were sampled using an oscilloscope as the ADC at the sampling rate of 80 GS/s with a vertical resolution of eight bits.

The Tx and Rx impairments were emulated digitally as arbitrary impairments were difficult to impose in the analog domain. In this experiment, we mainly focused on IQ skew in the Tx and Rx. IQ skew of X polarization from -10 to $+10$ ps in steps of 1 ps were imposed to the signal generated from the DAC and to those obtained with the ADC. For the condition of multiple impairments, we also evaluated the cases in which the IQ phase deviation of X polarization of 0° and $\pm 10^\circ$ was digitally emulated in the Tx and Rx. Strictly speaking, the IQ phase deviation imposed in this manner did not fully match the impairment model described in Section 2.1 if there remained IQ skew in the Tx and Rx devices, though they were calibrated as much as possible. Since the average amplitudes of IQ components are relatively easy to access in current Tx/Rx transceivers, we did not include IQ imbalance explicitly in this experiment. For each combination of impairments, the received waveforms were acquired three times.

DSP was carried out offline. The demodulation DSP was almost the same as that used in the above simulation, though pilot-based data-aided LMS was applied in this experiment. Pilot-based DSP was achieved as follows. After CD compensation, the pilot position was detected in accordance with the difference in the averaged powers between the 64QAM signal and QPSK pilot. Polarization demultipexing was then carried out using CMA for the pilot. Timing alignment of the received signal and pilot sequence was achieved using their correlation. With the timing alignment, the main DSP with the multi-layer SL&WL filters was applied to the signal before CD compensation again. The configuration of the multi-layer SL&WL filters were the same as in the simulation. The filter coefficients of the first, third, and fifth layers were adaptively updated using the QPSK pilot with data-aided LMS. The step sizes of the update were 10^{-3} for the first and fifth layers, and 10^{-2} for the third layer. After the adaptive multi-layer SL&WL filters, GSOP was carried out, then the pilot and overhead were removed to evaluate the normalized general mutual information (NGMI) as a performance indicator [28]. The amounts of IQ skew, IQ imbalance, and IQ phase deviation in the Tx and Rx were estimated using the WL filter coefficients of the first and the fifth layers as well.

Figure 7 shows the results of NGMI for all the $21^2 \times 3^2$ combinations of IQ skew and IQ phase deviation in the Tx and Rx and 3 acquisitions, simultaneously. The results are arranged as the function of IQ skew in the Tx in Fig. 7(a) and as that in the Rx in Fig. 7(b). The results with 2×2 SL are also plotted as a reference. With the multi-layer SL&WL filters, a stable NGMI of about 0.9 was obtained regardless of the impairments.

Figure 8 shows the results of the impairment monitoring for IQ skew of X polarization in the Tx and Rx. Similarly, the results for all combinations of IQ skew and IQ phase deviation in the Tx and Rx are plotted simultaneously, arranged as a function of IQ skew in Tx (Fig. 8(a)) and Rx (Fig. 8(b)), respectively. The monitored values are plotted on the left axis and the monitored

Optics EXPRESS

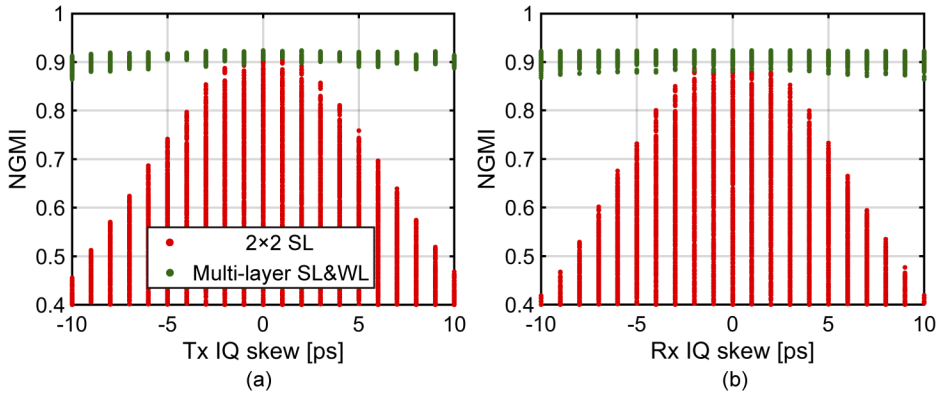

Fig. 7. Experimental results of NGMI with (a) Tx IQ skew and (b) Rx IQ skew. At each Tx (Rx) IQ skew, results of Rx (Tx) IQ skew from −10 to +10 ps and Tx/Rx IQ phase deviation of 0° and ±10° are plotted.

errors from the emulated values are plotted on the right axis. For IQ skew emulated in both the Tx and Rx, the estimated values corresponded to the emulated ones. The monitored errors were within ±0.5 ps. The results confirm that the impairments in both Tx and Rx could be individually monitored precisely and simultaneously from the WL filter coefficients in the multi-layer SL&WL filters adaptively controlled by SGD with back propagation. Since this monitoring scheme relies on pilot-based adaptive equalization, it can be used with probabilistic constellation shaping straightforwardly if pilot-based signal processing is adopted.

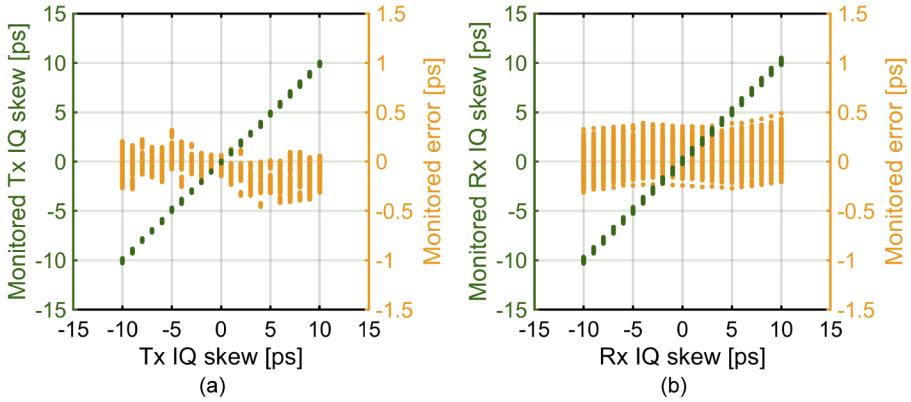

Fig. 8. Experimental results of impairment monitoring for (a) Tx IQ skew and (b) Rx IQ skew. At each Tx (Rx) IQ skew, results of Rx (Tx) IQ skew from −10 to +10 ps and Tx/Rx IQ phase deviation of 0° and ±10° are plotted.

5. Conclusion

We proposed a monitoring method for individual impairments in a Tx and Rx including IQ skew, IQ imbalance, and IQ phase deviation on the basis of the filter coefficients of our adaptive multi-layer SL&WL filter architecture controlled by SGD with back propagation. Considering the order in which IQ impairments occur in a Tx or Rx, the model relating IQ skew, IQ gain imbalance, and IQ phase deviation to the corresponding WL filter responses in the multi-layer filter architecture were obtained. The proposed method was evaluated through simulations using

Optics EXPRESS

32-Gbaud PDM-QPSK and a 100-km SMF transmission experiment of 32-Gbaud PDM-64QAM. The results indicate that IQ skew, IQ imbalance, and IQ phase deviation in both Tx and Rx could be individually monitored from the WL filter coefficients precisely and simultaneously when multiple impairments existed.

Appendix: Convergence speed under multiple impairments

We compared the convergence speed of the adaptive multi-layer SL&WL filters when multiple impairments existed. A learning curve of the loss of data-aided LMS at the pilot symbols, that is, the training loss is the indicator of the convergence performance. Figure 9 shows the time development of the training losses obtained in the 100-km SMF transmission experiment of 32-Gbaud PDM-64QAM. Even when multiple impairments existed, the convergence speed was little affected and the losses are almost converged after 2000 symbols.

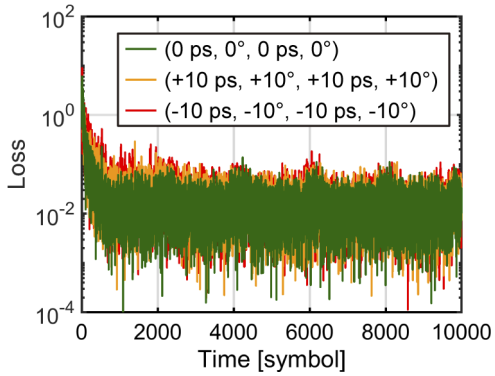

Fig. 9. Experimental results of time development of loss function. (Tx IQ skew, Tx IQ phase deviation, Rx IQ skew, Rx IQ phase deviation) are (0 ps, 0°, 0 ps, 0°), (+10 ps, +10°, +10 ps, +10°), and (−10 ps, −10°, −10 ps, −10°).

Funding. Ministry of Internal Affairs and Communications (JPMI00316); Ministry of Education, Culture, Sports, Science and Technology (19H02138).

Acknowledgments. We thank Masaki Sato and Emmanuel Le Taillandier de Gabory for their insightful discussions.

Disclosures. The authors declare no conflicts of interest.

References

1. S. Beppu, K. Kasai, M. Yoshida, and M. Nakazawa, "2048 QAM (66 Gbit/s) single-carrier coherent optical transmission over 150 km with potential SE of 15.3 bit/s/Hz," Opt. Express **23**(4), 4960–4969 (2015).
2. H.-C. Chien, J. Zhang, J. Yu, and Y. Cai, "Single-carrier 400G PM-256QAM generation at 34 Gbaud trading off bandwidth constraints and coding overheads," in *Optical Fiber Communication Conference* (2017), paper W1J.3.
3. A. Matsushita, M. Nakamura, F. Hamaoka, S. Okamoto, and Y. Kisaka, "High-spectral-efficiency 600-Gbps/carrier transmission using PDM-256QAM format," J. Lightwave Technol. **37**(2), 470–476 (2019).
4. F. Buchali, F. Steiner, G. Böcherer, L. Schmalen, P. Schulte, and W. Idler, "Rate adaptation and reach increase by probabilistically shaped 64-QAM: An experimental demonstration," J. Lightwave Technol. **34**(7), 1599–1609 (2016).
5. S. L. I. Olsson, J. Cho, S. Chandrasekhar, X. Chen, E. C. Burrows, and P. J. Winzer, "Record-high 17.3-bit/s/Hz spectral efficiency transmission over 50 km using probabilistically shaped PDM 4096-QAM," in *Optical Fiber Communication Conference* (2018), paper Th4C.5.
6. T. Kobayashi, M. Nakamura, F. Hamaoka, N. Nagatani, H. Wakita, H. Yamazaki, T. Umeki, H. Nosaka, and Y. Miyamoto, "35-Tb/s C-band transmission over 800 km employing 1-Tb/s PS-64QAM signals enhanced by complex 8 × 2 MIMO equalizer," in *Optical Fiber Communication Conference* (2019), paper Th4B.2.
7. X. Chen, J. Cho, A. Adamiecki, and P. Winzer, "16384-QAM transmission at 10 GBd over 25-km SSMF using polarization-multiplexed probabilistic constellation shaping," in *European Conference on Optical Communication* (2019), paper PD3.3.

Optics EXPRESS

8. K. Schuh, F. Buchali, W. Idler, T. A. Eriksson, L. Schmalen, W. Templ, L. Altenhain, U. Dümler, R. Schmid, M. Möller, and K. Engenhardt, "Single carrier 1.2 Tbit/s transmission over 300 km with PM-64QAM at 100 Gbaud," in *Optical Fiber Communication Conference* (2017), paper Th5B.5.
9. F. Buchali, M. Chagnon, K. Schuh, and V. Lauinger, "Beyond 100 Gbaud transmission supported by 120 GSa/s CMOS digital to analog converter," in *European Conference on Optical Communication* (2019), paper Tu.2.D.3.
10. M. Nakamura, F. Hamaoka, H. Yamazaki, M. Nagatani, Y. Ogiso, H. Wakita, M. Ida, A. Matsushita, T. Kobayashi, H. Nosaka, and Y. Miyamoto, "1.3-Tbps/carrier net-rate signal transmission with 168-Gbaud PDM PS-64QAM using analogue-multiplexer-integrated optical frontend module," in *European Conference on Optical Communication* (2019), paper Tu.2.D.5.
11. S. J. Savory, "Digital filters for coherent optical receivers," Opt. Express **16**(2), 804–817 (2008).
12. R. Kudo, T. Kobayashi, K. Ishihara, Y. Takatori, A. Sano, E. Yamada, H. Masuda, Y. Miyamoto, and M. Mizoguchi, "Two-stage overlap frequency domain equalization for long-haul optical systems," in *Optical Fiber Communication Conference* (2009), paper OMT3.
13. L. E. Nelson, G. Zhang, M. Birk, C. Skolnick, R. Isaac, Y. Pan, C. Rasmussen, G. Pendock, and B. Mikkelsen, "A robust real-time 100G transceiver with soft-decision forward error correction," J. Opt. Commun. Netw. **4**(11), B131–B141 (2012).
14. E. P. da Silva and D. Zibar, "Widely linear equalization for IQ imbalance and skew compensation in optical coherent receivers," J. Lightwave Technol. **34**(15), 3577–3586 (2016).
15. R. Rios-Müller, J. Renaudier, and G. Charlet, "Blind receiver skew compensation and estimation for long-haul non-dispersion managed systems using adaptive equalizer," J. Lightwave Technol. **33**(7), 1315–1318 (2015).
16. C. R. S. Fludger and T. Kupfer, "Transmitter impairment mitigation and monitoring for high baud-rate, high order modulation systems," in *European Conference on Optical Communication* (2016), paper Tu.2.A.2.
17. Q. Zhang, Y. Yang, C. Guo, X. Zhou, Y. Yao, A. P. T. Lau, and C. Lu, "Algorithms for blind separation and estimation of transmitter receiver IQ imbalances," J. Lightwave Technol. **37**(10), 2201–2208 (2019).
18. Y. Fan, Y. Jiang, J. Liang, Z. Tao, H. Nakashima, and T. Hoshida, "Transceiver IQ imperfection monitor by digital signal processing in coherent receiver," in *Optoelectronics and Communications Conference* (2019), paper ThC2-1.
19. J. Liang, Y. Fan, Z. Tao, X. Su, and H. Nakashima, "Transceiver imbalances compensation and monitoring by receiver DSP," J. Light. Technol. early access.
20. C. Ju, N. Liu, and C. Li, "In-service blind transceiver IQ imbalance and skew monitoring in long-haul non-dispersion managed coherent optical systems," IEEE Access **7**, 150051–150059 (2019).
21. I. Fatadin, S. J. Savory, and D. Ives, "Compensation of quadrature imbalance in an optical QPSK coherent receiver," IEEE Photonics Technol. Lett. **20**(20), 1733–1735 (2008).
22. M. Arikawa and K. Hayashi, "Adaptive equalization of transmitter and receiver IQ skew by multi-layer linear and widely linear filters with deep unfolding," Opt. Express **28**(16), 23478–23494 (2020).
23. Y. LeCun, Y. Bengio, and G. Hinton, "Deep learning," Nature **521**(7553), 436–444 (2015).
24. K. Kikuchi, "Fundamentals of coherent optical fiber communications," J. Lightwave Technol. **34**(1), 157–179 (2016).
25. K.-P. Ho, *Phase-modulated optical communication systems*, (Springer, 2005, Chap. 3).
26. K. Gregor and Y. LeCun, "Learning fast approximation of sparse coding," in *International Conference on Machine Learning* (2010), 399–406.
27. F. M. Gardner, "A BPSK/QPSK timing-error detector for sampled receivers," IRE Trans. Commun. Syst. **34**(5), 423–429 (1986).
28. J. Cho, L. Schmalen, and P. J. Winzer, "Normalized generated mutual information as a forward error correction threshold for probabilistically shaped QAM," in *European Conference on Optical Communication* (2017), paper M.2.D.2.